Journal of
Applied
Crystallography
ISSN 0021-8898

Received 24 June 2004
Accepted 5 October 2004

Focusing optics for molybdenum radiation: a bright laboratory source for small-molecule crystallography

Simon J. Coles* and Michael B. Hursthouse

School of Chemistry, University of Southampton, Hampshire SO17 1BJ, UK. Correspondence e-mail: s.j.coles@soton.ac.uk

This paper reports the design, installation and testing of a set of multilayer confocal mirrors in a side-by-side arrangement, built to increase the intensity from a molybdenum rotating-anode X-ray source. Ray-tracing experiments were performed in order to evaluate the best design parameters for the system, which are shown to be a side-by-side configuration of 100 mm length. Measurements of the primary beam intensity show an increase by a factor of approximately five. Comparative data collections were performed which highlight significant enhancements in the derived crystal structure, arising from the increased intensity of the primary beam.

1. Introduction

Developments in synchrotron science at dedicated central facilities, such as Station 9.8 (SRS, UK; Cernik *et al.*, 1997; http://srs.dl.ac.uk/xrd/9.8), XRD1 (Elettra, Italy; http://www.elettra.trieste.it/experiments/beamlines/xrd1/index.html) and ChemMatCARS (APS, USA; http://cars9.uchicago.edu/chemmat/forNNusers/chemhomenn.html), have allowed small-molecule crystallographers to study increasingly small crystals (Clegg, 2000, and references therein) and enabled experiments that are more complex and advanced (Helliwell, 2002). The huge difference in the capabilities of synchrotron facilities compared with the conventional facilities in the home laboratory has allowed chemical sciences to benefit greatly so that, in many cases, studies have been performed that otherwise would have been impossible. Indeed, these facilities are so successful that the three most recent synchrotrons to be commissioned have all included small-molecule diffraction stations in their design, to come on-line between 2004 and 2006 (Diamond Light Source, http://www.diamond.ac.uk/Activity/I19; Canadian Light Source, http://www.lightsource.ca/publications/activities_report.pdf; Australian Synchrotron, http://www.synchrotron.vic.gov.au/content.asp?Document_ID=449). However, centralized facilities are exceedingly expensive to run and maintain, and in some cases access to them can be difficult and time consuming to obtain.

In recent years, the macromolecular crystallography community has sought to develop hardware instrumentation in the home laboratory to reduce the gap between home and synchrotron facilities. The system of choice for a macromolecular laboratory is that of a rotating-anode generator, equipped with focusing mirrors, coupled to a sensitive area detector (Yang *et al.*, 1999). Mirrors have been used extensively at synchrotron sources for focusing X-rays for many years (Huxley & Holmes, 1997; Lienert *et al.*, 1998), and it is this principle that has been developed over the past decade or so for the home laboratory (Arndt, 1990). The primary drive for this development has been in the area of protein crystallography, and home-laboratory focusing mirrors operating in the 1.5–2 Å wavelength range have been in use in this domain for some time now. Indeed, an evaluation of the performance of such optics (Cu $K\alpha$ = 1.54 Å) revealed the enhancement gained from X-ray focusing (Kusz & Bohm, 2002).

It is now clear that the small-molecule crystallography community would also benefit from such advances in instrumentation in order to reduce the workload on oversubscribed synchrotron facilities and better screen candidate samples (Bond & Davies, 2003). The requirements of such work are different from those of the macromolecular community in that shorter-wavelength radiation is necessary (Mo $K\alpha$ as opposed to Cu $K\alpha$). Mo $K\alpha$ has a lower scattering power than Cu $K\alpha$ and a much lower efficiency (from the source) than Cu $K\alpha$. The required Bragg angles are half those of Cu $K\alpha$, thus necessitating half the capture angle of the X-rays from the source onto the optic. Until recently, the technology to address this issue had not been available.

This paper outlines the design, implementation and performance of a graded multilayer focusing optic for a molybdenum rotating-anode generator.

2. Design

A ray-tracing study was performed by Osmic Inc. to establish the optimal design for a set of focusing multilayer optics [Confocal Max-Flux (CMF) optics] to be coupled to a Bruker Nonius FR591 rotating-anode generator. A series of simulations was performed for a conventional graphite monochromator and CMF optics of lengths 80 and 100 mm. The X-ray flux at the crystal position was computed for a range of

instrument variables, such as power settings, source size and pinhole size, in order to discover the optimum length and design for the optic.

The first factor to influence the design is the beam size at the crystal, which determines the performance of the system for different samples. Fig. 1 shows the intensity relative to that of the graphite monochromator as a function of pinhole size for the 80 (CMF-13-23Mo8) and 100 mm (CMF-14-24Mo10) optics. As CMF optics form a small but bright beam at focus, the intensity gain for a small sample is larger than that for a large sample. Different pinhole sizes are used for investigating the performance for different sample sizes.

The source size and power settings were also considered. A 0.3 mm source (5 kW) was used for simulating the performance of the graphite monochromator, whilst both 0.3 and 0.2 mm sources were used for investigating the CMF optic performance. Because of the bandpass nature of the CMF optics, a smaller, but brighter, source delivers a better performance. The original instrument design of a source size of 0.3 mm and a power setting of 5 kW was retained for the experiment. Table 1 shows the performance results for both the 80 and the 100 mm CMF optics for the chosen source and pinhole sizes. This setup produces a flux gain relative to that of the graphite monochromator of 2.63 and 3.81 for the 80 and 100 mm CMF optics, respectively, and hence the 100 mm optic (CMF-14-22Mo10) was chosen as the best design. The calculations show a fourfold increase in flux for these mirrors; however, the calculations cannot take into account factors such as actual source intensity distribution (which is affected by the anode surface, the bias *etc.*) and the efficiency of the original monochromator, which will all affect the actual intensity gain. The graphite monochromator in the simulation was assumed to have a nearly perfect performance (a mosaicity of 0.4° and a peak reflectivity of 45%).

Table 1
Comparative performance between 80 (CMF13-23Mo8) and 100 mm (CMF14-22Mo10) confocal optics.

	CMF13-23Mo8	CMF14-22Mo10
FWHM at focus (mm)	0.07	0.07
FWHM at pinhole (mm)	0.13	0.14
FWHM at sample (mm)	0.07	0.07
FWHM at detector (mm)	0.26	0.33
FW10% at focus (mm)	0.15	0.15
FW10% at slit 2 (mm)	0.28	0.29
FW10% at sample (mm)	0.13	0.13
FW10% at detector (mm)	0.39	0.47
System effective efficiency	1.13×10^{-7}	1.64×10^{-7}
Photons per second	2.82×10^{7}	4.11×10^{7}
$K\beta/K\alpha$ ratio	5.69×10^{-4}	6.30×10^{-4}
Divergence (°)	0.24	0.31

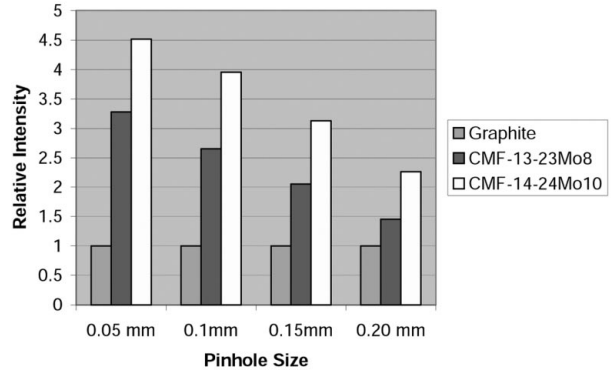

Figure 1
Intensity enhancement for 80 and 100 mm optics, relative to a graphite monochromator, at pinhole settings of 0.05, 0.1, 0.15 and 0.2 mm.

3. Implementation and performance

A multilayer is a thin-film coating on substrate composed of alternating layers of high and low electron density. The mirrors may be manufactured by vacuum deposition techniques, such as sputtering, chemical vapour deposition or molecular beam epitaxy. The mirrors are built in a side-by-side geometry perpendicular to each other, as shown in Fig. 2 (Verman *et al.*, 1998). Also shown in Fig. 2 is a schematic of the focusing geometry of this arrangement; it can be seen that a double bounce of the X-ray beam on the mirror causes a focusing effect. For a maximum gain in intensity, the system was designed with the mirrors as close as possible to the source, and to focus at the crystal. In addition, an intrinsic property of multilayer Bragg reflection is that the mirrors monochromate the incident beam, whilst discriminating between harmonics. The mirrors are then mounted in a sealed housing, so that they may be evacuated in order to reduce air scatter, and are equipped with vertical and horizontal translators to facilitate alignment. This housing is then mounted on the shutter port of the anode, as shown in Fig. 3.

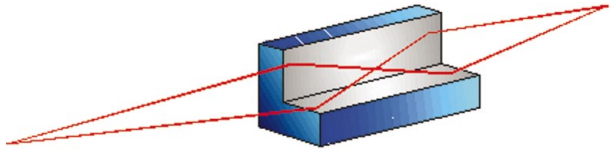

Figure 2
The 'side-by-side' arrangement of CMF optics, showing the 'double bounce' focusing effect (Verman *et al.*, 1998).

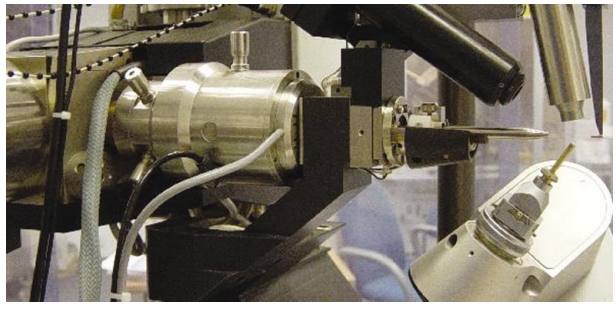

Figure 3
The confocal optic installation on the KappaCCD rotating-anode system.

Table 2
Comparison of data and structure quality between the two systems.

	Graphite monochromator	CMF14-22Mo10
Angular range covered (°)	343	356
Maximum theta angle (°)	27.48	27.39
No. of measured reflections	19 655	17 853
No. of independent reflections	6924	6374
No. of reflections > 4σ	3923	5781
Completeness	95.8%	88.4
R_{int}	0.0978	0.0464
R_1, wR_2 (observed data)	0.0598, 0.0919	0.0388, 0.0982
R_1, wR_2 (all data)	0.1382, 0.1098	0.0461, 0.1104

The increase in intensity obtained from the installation of the 100 mm confocal optics was measured by recording the flux density at the sample position and comparing the diffracted intensities by recording data on a test crystal. The comparison measurements were made with the confocal mirror system described above *versus* those made with the same operational parameters on a Huber 151 flat monochromator (crystal size 12 × 12 mm; reflection plane 002; mosaic spread 0.4°; FWHM 0.1°).

As a primary measure of the difference in performance of the two monochromating systems, the intensity of the main beam at the crystal diffracting position was recorded. A two-dimensional CCD detector was used to measure the intensity profile in the horizontal and vertical directions (Fig. 4). These results clearly show the increase in intensity by a factor of five of the confocal optics over the conventional graphite monochromator. Moreover, a significant reduction (> 50%) in the FWHM is observed for the mirror configuration, indicating a high degree of focusing and hence a reduction in air scatter compared with the larger beam produced by the monochromator.

As a gauge of the impact of an increased intensity source on the quality of a structure determination, data were measured on a test crystal both before (with the graphite monochromator) and after installation of the optics. The crystal was selected on the basis of its diffracting power, such that the diffraction pattern was reasonably intense on the graphite system but did not overload the detector on the confocal system when exposed for the same duration. The full details of the structure determination of this sample have been published elsewhere (Pla-Quintana *et al.*, 2004).

Table 2 compares the data obtained for the monochromator and the mirrors. CIFs and details of the data-collection parameters have been deposited for both data sets as supplementary material.[1] Moreover, all the digital information generated during the course of both these structure determinations is available on a public open access crystal structure archive so that the reader may fully assess the difference between the two experiments. Data pertaining to the graphite and mirror data collections may be found at http://ecrystals.chem.soton.ac.uk/143 and http://ecrystals.chem.soton.ac.uk/144, respectively. Data-collection parameters such as detector distance (45 mm), scan time (150 s) and scan increment (1°) were the same for both collections, and the coverage was made as consistent as possible. The crystal was a platelet of dimensions 0.1 × 0.08 × 0.01 mm glued onto a glass fibre.

These results show that, despite a reduced completeness of the data set, the structure obtained using the mirror system has an agreement factor some 2% lower than that from the conventional monochromator, presumably as a result of the dramatic increase (nearly 50%) in the number of observed reflections.

A visual representation of the enhancement of the intensity of the beam can be seen in the simulated precession photographs in Fig. 5. These simulations show the diffraction patterns for both samples in the *h*0*l* plane and are generated directly from the collected images. Both patterns are therefore created under identical experimental conditions and it is clear that the diffracted intensity from the mirror system is much greater.

A quantitative comparison of the error in the two different data sets is shown in Fig. 6, which depicts a scatterplot of the standard uncertainty for a particular measurement against the measured value for that particular measurement for both complete data sets. A considerably more acceptable agreement factor is observed for the mirror system than for the graphite monochromator, indicating that a significantly more accurate measurement has been performed by the former system.

A more rigorous statistical comparison of the enhancement in the intensity of the beam was performed in order to obtain a more quantitative estimate. The results are shown in the half normal probability plots of Figs. 7 and 8. A half normal probability plot (HNPP) (Abrahams & Keve, 1971) may be used as an indicator of the degree of similarity between two data sets, taking into account the standard uncertainties on the measurements, and is defined as follows:

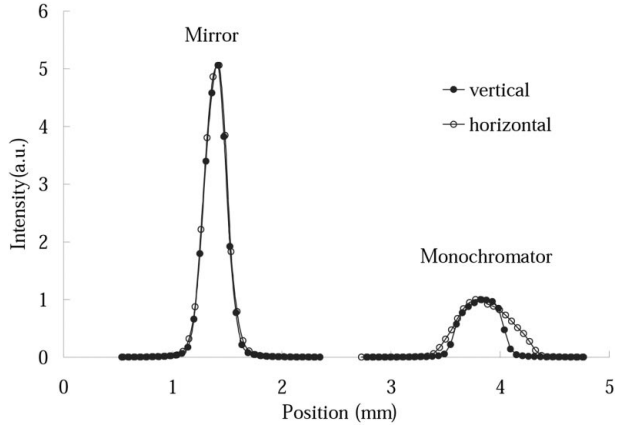

Figure 4
A comparison of vertical and horizontal beam intensity profiles for the two systems.

[1] Supplementary data for this paper are available from the IUCr electronic archives (Reference: AJ5028). Services for accessing these data are described at the back of the journal.

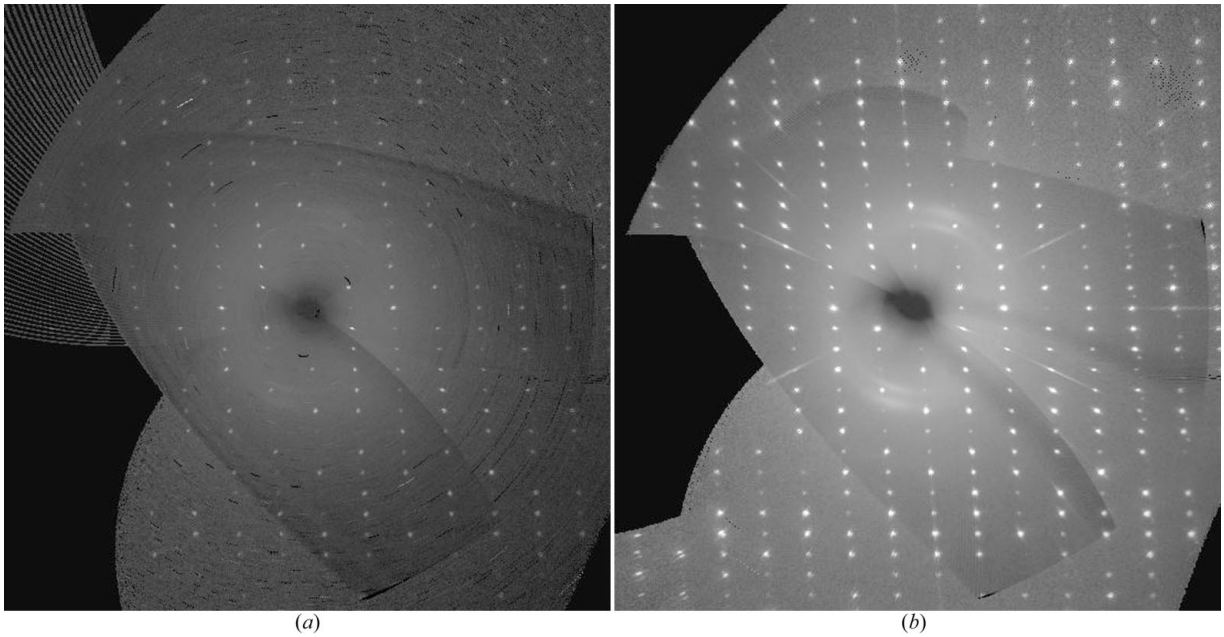

(*a*) (*b*)

Figure 5
Simulated precession images of the *h*0*l* layer for (*a*) the graphite monochromator and (*b*) the confocal optic systems.

$$\left|\delta_i\right| = \left|v_1 - v_2\right| / \left[\sigma^2(v_1) + \sigma^2(v_2)\right]^{1/2},$$

where δ_i is computed, ordered and plotted against those expected for a standard half normal distribution. A linear HNPP with a slope of unity and intercept of zero indicates a correct match between the measured and assumed distribution, with correctly estimated standard uncertainties. A deviation of the slope from unity shows a difference between the two measurements, whilst a non-zero intercept is indicative of underestimated standard deviations.

HNPP studies were carried out on a randomly chosen subset of both the intensity (*hkl*) data sets (Fig. 7) in order to highlight differences in the beam diffracted by the crystal. From this plot it can be seen that the slope is linear but deviates significantly from unity. This result indicates a considerable difference in the intensity of the diffracted beam produced by the two systems. A non-zero intercept also indicates that the standard uncertainties of one or both of the data sets have been underestimated, although this is known to be a common problem with area-detector data (Martin & Pinkerton, 1998).

Furthermore, an HNPP was generated as a study of the differences between the two derived structures. This was performed by comparison of bond lengths and is shown in Fig. 8. The effects of the increased beam intensity on the derived structure can be seen here as a considerable deviation from linearity. Moreover, the slope exhibits a significant departure from unity, which is presumably an enhancement of the highlighted differences in the diffracted intensities. The two structures are shown here to be significantly different, and again there is an underestimation of the standard uncertainties.

Perhaps the best indicator of the impact of focusing mirrors on the operation of a home laboratory is the number of failed samples on the instrument. The instrument on which the confocal mirrors for Mo radiation are installed is operated by

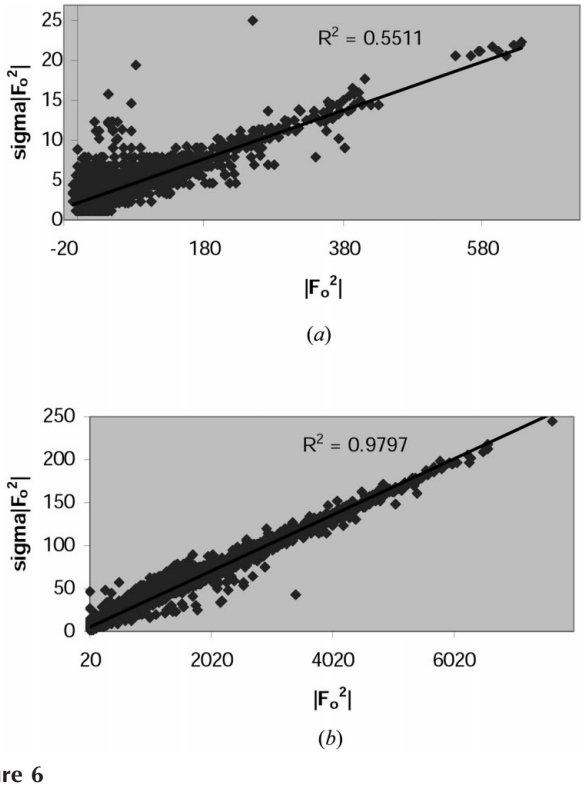

Figure 6
Plots of the standard uncertainty of a measurement against the value of that measurement for (*a*) the graphite monochromator and (*b*) the confocal optic systems.

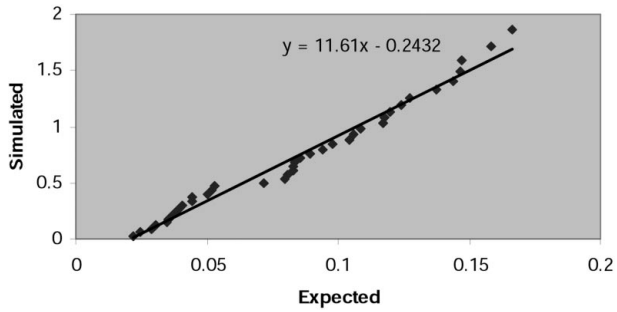

Figure 7
A half normal probability plot comparing diffracted beam intensities.

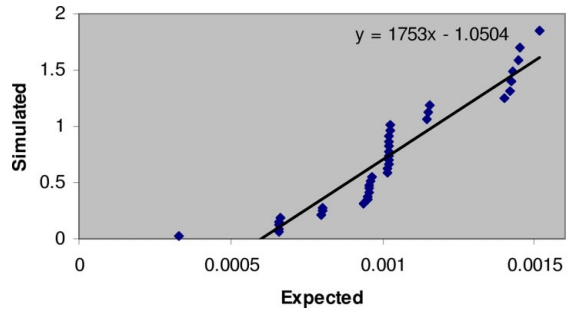

Figure 8
A half normal probability plot comparing derived geometries.

the UK National Crystallography Service (UK–NCS). The laboratory service serves as a screen for a further synchrotron service. Whilst running this extended synchrotron service, it was observed that in the 2.5 years prior to mirror installation the percentage of samples submitted to the UK–NCS that needed to be referred to the synchrotron service was on average 20%. In the nine months since the installation of these mirrors, the referral rate has dropped dramatically to 4.5%. This statistic is possibly more important when considering that the UK–NCS processes in excess of 1000 samples per annum.

4. Conclusion

This paper presents the successful design, installation and implementation of the first focusing optics for a molybdenum rotating-anode X-ray generator for small-molecule crystallography. This system has been shown to increase the intensity of the incident X-ray beam on a sample by a factor of five, with a resulting increase in data quality. This effect has enabled the successful study of very small and weakly diffracting crystals that hitherto has proved to be very challenging or indeed impossible on laboratory sources. This system also serves to reduce the difference between the beam intensities of the home laboratory and synchrotron sources, thus providing an enhanced screening mechanism and reducing the workload at these facilities.

The authors thank Osmic Inc., Bruker Nonius BV and Incoatec GmbH for contributions and assistance in making this experiment a success.

References

Abrahams, S. C. & Keve, E. T. (1971). *Acta Cryst.* A**27**, 157–165.
Arndt, U. W. (1990). *J. Appl. Cryst.* **23**, 161–168.
Bond, A. D. & Davies, J. E. (2003). *Chem. Br.* **39**, 44.
Cernik, R. J., Clegg, W., Catlow, C. R. A., Bushnell-Wye, G., Flaherty, J. V., Greaves, G. N., Burrows, I., Taylor, D. J., Teat, S. J. & Hamichi, M. (1997). *J. Synchrotron Rad.* **4**, 279–286.
Clegg, W. (2000). *J. Chem. Soc. Dalton Trans.* **19**, 3223–3232.
Helliwell, J. R. (2002). *J. Synchrotron Rad.* **9**, 1–8.
Huxley, H. E. & Holmes, K. C. (1997). *J. Synchrotron Rad.* **4**, 366–379.
Kusz, J. & Bohm, H. (2002). *J. Appl. Cryst.* **35**, 8–12.
Lienert, U., Schulze, C., Honkimaki, V., Tschentscher, T., Garbe, S., Hignette, O., Horsewell, A., Lingham, M., Poulsen, H. F., Thomsen, N. B. & Ziegler, E. (1998). *J. Synchrotron Rad.* **5**, 226–231.
Martin, A. & Pinkerton, A. A. (1998). *Acta Cryst.* B**54**, 471–477.
Pla-Quintana, A., Roglans, A., Torrent, A., Moreno-Manas, M. & Benet-Buchholz, J. (2004). *Organometallics*, **23**, 2762–2767.
Verman, B., Jiang, L., Kim, B., Smith, R. & Grupido, N. (1998). *Adv. X-ray Anal.* **42**, 321–327.
Yang, C., Courville, A. & Ferrara, J. D. (1999). *Acta Cryst.* D**55**, 1681–1689.